ResearchGate

See discussions, stats, and author profiles for this publication at: https://www.researchgate.net/publication/284281963

Influence of Krypton Seeding on DD Fusion Neutron Production: Evaluation Methodology for Plasma Focus Optimization

Article *in* Journal of Fusion Energy · November 2015

DOI: 10.1007/s10894-015-0041-2

CITATIONS
0

READS
108

8 authors, including:

Rishi Verma
Bhabha Atomic Research Centre
57 PUBLICATIONS **230** CITATIONS
SEE PROFILE

Paul Lee
National Institute of Education (NIE), Singa…
319 PUBLICATIONS **3,805** CITATIONS
SEE PROFILE

Stuart Victor Springham
National Institute of Education (NIE), Singa…
158 PUBLICATIONS **1,404** CITATIONS
SEE PROFILE

R.S. Rawat
National Institute of Education (NIE), Singa…
286 PUBLICATIONS **2,759** CITATIONS
SEE PROFILE

Available from: Sing Lee
Retrieved on: 15 September 2016

J Fusion Energ
DOI 10.1007/s10894-015-0041-2

ORIGINAL RESEARCH

Influence of Krypton Seeding on DD Fusion Neutron Production: Evaluation Methodology for Plasma Focus Optimization

A. Talebitaher[1] · S. Lee[3,4,5] · S. M. P. Kalaiselvi[2] · R. Verma[6] · P. Lee[2] · S. V. Springham[2] · T. L. Tan[2] · R. S. Rawat[2]

© Springer Science+Business Media New York 2015

Abstract A sub-kilo-Joule plasma focus device (FMPF-3, 14 kV/235 J) was operated with deuterium–krypton admixtures (of 1, 2 and 5 % Kr by volume) to study the influence of admixture ratio on neutron yield (Y_n). Experiments were performed for different insulator sleeve lengths and cathode geometries. The results reveal that for a carefully optimized electrode geometry the highest average neutron yield is obtained with pure deuterium as the operating gas, whereas krypton seeding leads to a reduction in Y_n. We argue that the electrode geometry and electrical coupling play critical roles in determining the influence of gas admixtures; and that for an optimized plasma focus device D_2-Kr admixtures may give little or no neutron yield enhancement relative to pure D_2 operation and so the admixture operation is an evaluation methodology to determine the level of optimization of device geometry.

✉ R. S. Rawat
rajdeep.rawat@nie.edu.sg

1 Energy Research Institute, Nanyang Technological University, 1 CleanTech Loop, Singapore 637141, Singapore

2 Natural Sciences and Science Education, National Institute of Education, Nanyang Technological University, 1 Nanyang Walk, Singapore 637616, Singapore

3 Institute for Plasma Focus Studies, 32 Oakpark Drive, Chadstone, VIC 3148, Australia

4 INTI International University, Nilai, Malaysia

5 University Malaya, Kuala Lumpur, Malaysia

6 Bhaba Atomic Research Centre, Autonagar, Visakhapatnam 530012, India

Keywords Miniature plasma focus device · Fusion reaction · Neutron source · Admixture gas · Neutron yield enhancement

Introduction

One of the main applications of the plasma focus (PF) device is as a pulsed neutron source using deuterium as the operating gas [1, 2]. The scaling of neutron yield (Y_n) with stored energy and peak discharge current has been investigated for various PF devices [3]. However, for a specific device with a given storage energy, the neutron yield can be optimized through selection of parameters for the electrode assembly geometry [4–6]. Different groups have investigated the influence of the high-Z gases (admixed with deuterium) on neutron yield, and concentrating mainly on their role in the formation of micro-pinches [7] or super-dense domains [8], stabilized pinch column effects [9, 10] and promotion of slipping of the current sheath near the anode surface due to the Hall effect [11]. Verma et al. [12] investigated the correlation between neutron yield and hard X-ray emission, and concluded that the addition of high-Z gases resulted in higher radiation emission, tighter compression and therefore a smaller final pinch radius [13, 14]. According to these authors, the higher plasma density in the radiatively-collapsed pinched column for deuterium–krypton admixture operation leads to neutron yield enhancement. For the 200 J FMPF-1 device [12], they reported a maximum of 30-fold increase in Y_n: from $(1.0 \pm 0.3) \times 10^4$ to $(3.1 \pm 0.4) \times 10^5$ n/shot. The experimental results on fusion source (proton) imaging, by Springham et al. [15] on the NX2 PF device clearly showed that D_2-Kr admixtures resulted in a smaller source size than is the case for pure D_2 operation. However, unlike the

Published online: 20 November 2015

associated X-ray images, the fusion images showed no evidence for the existence of hot spots, micro-pinches or $m = 0$ instabilities.

Babazadeh et al. [6] observed an increase in neutron yield by a factor of 3.5 for krypton admixture operation of a 90 kJ Filippov type PF device (flat insert on anode end), while the factor was 1.5 for a conical insert on the same anode (of length 15.5 cm). This indicates that the enhancement factor is dependent upon the device electrode geometry: especially the anode size and shape. In addition, for pure D_2 operation the measured neutron yield with the conical insert was about six times greater than that for the flat anode; indicating that the yield enhancement obtained from krypton seeding is less significant for well-optimized PF anode geometries. Moreover, with the same 90 kJ Filippov device, but with a shorter (11 cm) anode, Mohammadi et al. [16] found an order of magnitude increase in neutron yield with krypton admixtures. However, the maximum yield achieved with 3 % krypton seeding was of similar magnitude to that obtained by Babazadeh et al. [6] with a flat anode (non-optimized case).

However, not all the relevant experimental data accords with a neutron yield enhancement in the presence of a high-Z impurity. For example, Bures et al. [4] replaced the cylindrical anode with a conical anode and showed a significant improvement in neutron yield. However, when different percentages of Ar and Kr were added to the D_2 gas, the cylindrical anode case showed an enhancement of neutron yield while the conical anode case did not. Rossel and Choi [17] used the DPF-78 device (60 kV, 28 kJ) with different admixtures of noble gases (Ne, Ar or Kr with D_2) and found a reduction in neutron yield for all admixture ratios. Furthermore, no correlation was observed between the total neutron yield and the hard X-ray emission or the appearance of hot spots.

In this study, we try to find a correlation between the influence of krypton seeding and the neutron yield of an "optimized" and "non-optimized" PF device. An optimized PF device is the device that produces maximum neutron yield. The optimized PF operation, with maximum neutron yield, is normally achieved after a large number of experimental iterations by optimizing device and operating parameters such as length and material of insulator sleeve, cathode and anode radii, length and material of anode, deuterium gas pressure, etc. for fixed energy storage and discharge current values. For example, the initial efforts on FMPF-1 device with tubular cathode geometry and different anodes gave the neutron yield of about 10^4 neutrons per shot [12, 18], which upon further optimization of anode shape, dimension and material increased the neutron yield to about 1.7×10^5 neutrons per shot [19]. The maximum neutron yield of about 1.0×10^6 neutrons per shot was finally achieved for FMPF-1 device by changing the tubular cathode geometry to squirrel cage geometry for the same set of anode [19]. Hence, the FMPF-1 device in references [12] and [18] was "non-optimized"; which was finally "optimized" with maximum neutron yield in Ref. [19].

The obvious question here is how one would know that the FMPF-1, or any other PF, device is eventually optimized or not for producing maximum neutron yield. One simple way would be to check whether the neutron yield is in line established neutron yield scaling laws or not. This, however, would only roughly tell whether one is close to optimized PF configuration, moreover the accuracy of extent of optimization simply depend on the extent of optimization achieved on reference PF device used for calibration. In this study, we propose that the effect of krypton seeding of deuterium on the neutron yield of PF device can be used to evaluate extent of PF optimization.

Experimental Setup and Results

This paper investigates the influence of krypton gas admixture on DD fusion neutron production from the FMPF-3 plasma focus device [20] which has recently been refurbished with new Pseudo Spark Gap (PSG) switches (Thyratron TDI1-200 kA/25 kV: Pulsed technologies Ltd., Russia). The 2.4 μF FMPF-3 is 4-module system with each of the 0.6 μF module, made up of two parallel 0.3 μF capacitors, connected to the plasma focus load through a 150 kA/25 kV PSG switch. The synchronized operation of PSG switches for all four modules is obtained using indigenously designed 4-channel heating system (for controlling the Hydrogen gas pressure inside each of the PSG switches) and a high performance 4-channel Blumlien pulser based triggering system of high repetition rate (10 Hz), low rise time (\10 ns) and low jitter (±1 ns). The use of 4-module system leads to lower total inductance about &34 ± 2 nH for FMPF-3 device. The 2.4 μF capacitor bank was charged to 14 kV (235 J) to achieve a peak discharge current of ~100 kA. A hollow tapered copper anode (shown in Fig. 1) of 20 mm length (12 mm diameter at the bottom, tapering to 8 mm at the top) was used for all experiments. Two different insulator sleeves of 5 and 10 mm effective length (the length that protrudes above the cathode plate) have been used to investigate the influence of insulator length on neutron yield. Also for the last part of experiment, the cathode rods were removed to test a different geometry from the conventional situation to give an example of another non-optimized geometry and to show how the krypton seeding enhances the neutron yield for that. For each group of experiments, the operating pressure was scanned from 2 to 14 mbar to find out the optimum pressure for the highest neutron yield. All

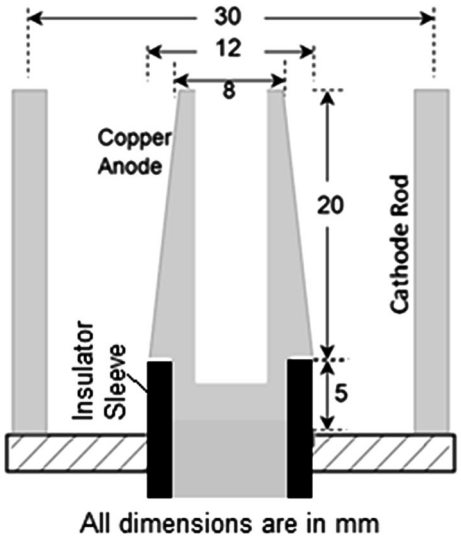

Fig. 1 Schematic of FMPF-3 electrode assembly. For the experiments in sections "Neutron Yield for 10 mm Insulator Sleeve" and "Neutron yield for Cathode-Less Geometry" an insulator with 10 mm length has been used

experiments were performed in static gas fill mode with the deuterium gas being filled at the desired gas pressure.

To measure the time-integrated neutron yield a sensitive He-3 proportional counter with Paraffin-wax moderator was positioned in the radial direction at 50 cm from the PF anode. This He-3 detector was cross-calibrated against a beryllium fast-neutron activation counter [21] using a PF with a higher neutron yield (NX2 device).

Neutron Yield for Pure Deuterium Operation for 5 mm Insulator Sleeve

In the first group of experiments, a series of measurements (each comprising a 55 shot series, fired at ~0.2 Hz) were performed using 5 mm long insulator sleeve for pure deuterium as the working gas. This series of experiments were done to verify the results obtained earlier by Verma et al. [20] where the maximum neutron yield was reported to be about $(1.5 \pm 0.2) \times 10^6$ n/shot on the similar device but with a slightly shorter anode length. It should however be pointed out that the charging voltage was increased from 13 kV, used in [20], to 14 kV in the present experiment. Consequently, the anode length was increased from 17 to 20 mm to compensate for the higher plasma sheath acceleration resulting from this higher charging voltage. The operating pressure was scanned from 2 to 14 mbar in steps of 1 mbar. As seen in Fig. 1, the shot-averaged neutron yield reached its maximum value of $Y_n = (1.8 \pm 0.4) \times 10^6$ n/shot at 8 mbar, and Y_n remained above 1.0×10^6 n/shot for a comparatively wide range of pressures (5–10 mbar). The results match well with the results obtained by Verma et al. [20]. Furthermore, the neutron yield is found to follow the empirical scaling law $Y_n \sim I^{3.4}$ [3] reasonably well.

Neutron Yield for Admixture Gas Operation for 5 mm Insulator Sleeve

In the second group of experiments, with the same PF geometry, krypton gas was mixed with deuterium in volumetric ratios of 1, 2 and 5 % to investigate the effect of high-Z gas admixture on neutron yield. For each gas admixture ratio, the "pressure scanning" was performed in the 2–14 mbar range. The average neutron yield was measured over a series of 55 shots fired using the same ~0.2 Hz repetition rate. As seen in Fig. 2, the optimum pressure remained at 8 mbar for 1 and 2 % krypton seeding with enhancements of the average neutron yield of ~60 % ($Y_n = (2.9 \pm 0.3) \times 10^6$ n/shot) for 1 % Kr, and ~20 % ($Y_n = (2.2 \pm 0.3) \times 10^6$ n/shot) for 2 % Kr. By contrast, a 65 % reduction in the average neutron yield ($Y_n = (6.2 \pm 0.3) \times 10^5$ n/shot) along with a reduction in optimum pressure to 6 mbar was found for 5 % Kr seeding. These results are markedly different from those of Verma et al. [12] for their experiments on the first version of this device, FMPF-1 (200 J, 2.4 μF, 27 nH, T/4 ~ 400 ns). The electrode assembly consisted of a 17 mm long stainless steel anode of composite geometry (tapered over the last 7 mm with diameter decreasing from 12 to 6 mm) and the chamber wall of 30 mm inner diameter acting as cathode. An insulator sleeve of Pyrex glass with a breakdown length of 5 mm was used. In that work, average neutron yield enhancement factors of 30, 20 and 1.2 were obtained for krypton seeding of 2, 5 and 10 %, respectively. For example, the neutron yield for pure deuterium operation at 3 mbar was $(1.0 \pm 0.3) \times 10^4$ n/shot, but increased to $(3.1 \pm 0.4) \times 10^5$ n/shot for 2 % Kr at the same pressure.

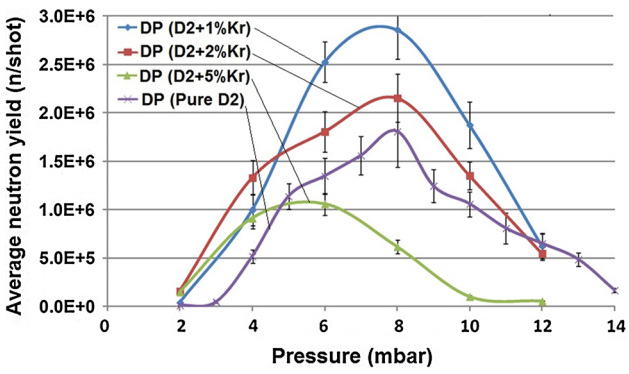

Fig. 2 Average neutron yield for 55 shots (per data point) with pure deuterium and D_2-Kr admixtures with 1, 2 and 5 % volumetric ratio of Kr. The anode length is 20 mm and insulator sleeve length is 5 mm

It is worth pointing out here that the admixture-related 30-fold enhancement in neutron yield for the FMPF-1 device was obtained before the geometry of the electrode assembly had been fully optimized. Subsequent to the work reported in references [12] and [18], the neutron yield was enhanced from 10^4 n/shot to 10^5 n/shot by fine-tuning the electrode assembly shape and dimensions with tubular cathode geometry, and finally to yields of 10^6 n/shot by simply implementing the squirrel-cage cathode configuration [19]. Hence, it is evident that the geometrical optimizations of the FMPF-1 electrodes led to a significantly greater increase in neutron yield than that obtained with deuterium–krypton admixtures. Unfortunately, the krypton admixture experiment was not done on improved version of FMPF-1 to test the influence of krypton seeding (and this device is not available anymore), however it obviously shows how geometrically optimization increase the fusion reaction, perhaps by increasing the average deuterons energy and optimized deuterium density distribution. In this situation, high-Z doping may reduce the DD reaction by cooling the pinch region (higher radiation) and consequently reducing the average deuteron energy.

The FMPF-3 device is an electrically upgraded version of FMPF-1 with a lower system inductance, and hence, a higher peak discharge current for the same operating voltage. For the FMPF-1 (latest version) and FMPF-3 devices in well-optimized configurations, the highest average neutron yields for pure D_2 operation and 200 J stored energy are 1.15×10^6 and 1.50×10^6 n/shot [20], respectively; hence a 30 % difference in favor of the FMPF-3. The peak discharge currents of the FMPF-1 and FMPF-3 devices are approximately 87 and 103 kA, respectively, at 14 kV operating voltage [22]. Therefore, from the $Y_n \sim I^{3.4}$ scaling law one would expect the FMPF-3 neutron yield to be approximately 80 % greater than that for FMPF-1 (if at least, FMPF-1 is considered as an optimized device). This indicates that some further optimization of the electrode geometry in FMPF-3 is possible. Table 1 shows the characteristics of two devices and their experimental average neutron yield. For 1 % krypton seeding in FMPF-3 the neutron yield is enhanced to a maximum of $(2.9 \pm 0.3) \times 10^6$ n/shot (refer to Fig. 1) which confirms that this device's performance with Kr seeding is at par with FMPF-1.

It is assumed that the krypton seeding enhances the density of pinch, (except for very high pressure) by making the pinch more compressible by the dual effect of radiative-cooling [23] and specific heat ratio (SHR) [24]. The krypton ions are not fully ionized thus contributing an inordinate proportion to the thermodynamic degree of freedom of the ensemble, which reduces the SHR of the mixture to significantly less than 5/3 of pure deuterium case [23, 24]. The voltage drop in the dI/dt signal (referred here as "depth of pinch") shown in Fig. 3 is a good indication of pinching efficiency for the given geometry.

Figure 2 shows an enhancement of 60 and 30 % in the "depth of pinch" for 1 and 2 % Kr-seeded respectively. This relatively low level of enhancement agrees with a computations based on the Lee model code [25] incorporating Kr-seeded thermodynamics, which predict neutron yield enhancements typically of tens of percent.

Springham et al. [15], in Figs. 2 and 3 of their paper, showed the different shape and size of the fusion source in pure deuterium and D_2-Kr admixture operation. For pure deuterium, the long and wide cone-shaped fusion source region is associated with forwardly directed high-energy deuteron beams, whereas, the compact prolate ellipsoid shaped fusion source observed for Kr-seeded operations indicates greater confinement of the fusion source. We conclude that krypton seeding plays dual and opposing roles in PF fusion. Firstly, Kr-seeding promotes better confinement of the fusion source and thereby increases the ion density and interaction probability, leading to an increased thermonuclear fusion neutron yield from the better confined pinched plasma for geometrically non-optimized devices. Secondly, the Kr-seeding promotes the radiative cooling of the pinch plasma resulting in lowering of the average kinetic energy of deuterons (in deuterium beam) and hence DD reaction cross-section would decrease which will lead to reduction in neutron yield by beam-target mechanism. Hence, Kr-seeding decreases the reaction yield for geometrically well-optimized devices as for them the beam-target mechanism is the dominant mechanism of neutron production. Furthermore, in the case of pure deuterium, all collisions (between beam deuteron and gas target) are DD, whereas in the doped case some collisions are D-Kr, which naturally decreases the neutron yield. To summarize, the average deuteron beam energy

Table 1 Characteristics of FMPF-1 and FMPF-3 and their neutron yield

	FMPF-1	FMPF-3
Circuit inductance (nH)	27	34
Circuit impedance (mΩ)	66	23
Peak current (I)	87 kA at 14 kV	103 kA at 14 kV
Neutron yield	1.0×10^4 (first version) 1.15×10^6 (latest version)	1.50×10^6
Scalable ($Y_n \sim I^{3.4}$)		2.04×10^6

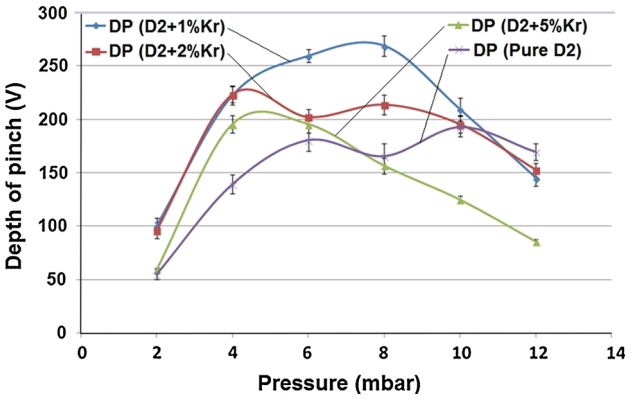

Fig. 3 Average depth of pinch for 55 shots (per data point) with pure deuterium and D_2-Kr admixtures with 1, 2 and 5 % volumetric ratio of Kr for 5 mm insulator sleeve length

and deuterium number density in pinch region both influence neutron yield. Krypton seeding will increase the deuterium number density by tighter pinch and better confinement resulting in higher thermal neutron yield, however the higher radiation losses results in reduction of average deuteron energy leading to lowering of beam-target neutron yield.

For "non-optimized" plasma focus device both of these parameters are not optimized i.e. deuterium number density in pinch is low due to inefficient pinch and average deuteron beam energy is also low compared to optimized value of about 100 keV; whereas for the "optimized" plasma focus device these parameters are close to their optimized values. For "non-optimized" device the relative increase in the deuterium number density due to increased confinement by Kr seeding is much higher than the decrease in average deuteron beam energy due to increased radiative cooling by Kr-seeding. In other words, the increased deuterium number density effect dominates over the reduced average deuteron energy for "non-optimized" device resulting in increased neutron yield. For "optimized" device the relative decrease in average deuteron energy is higher or comparable to relative increase in deuterium number density upon Kr-seeding leading to decrease in neutron yield.

It is also pertinent to compare the Speed Factor ($SF = (I/a)/\rho_0^{0.5}$, where I is the peak discharge current, α is the anode radius and ρ_0 is the optimum pressure giving the highest average neutron yield) for the FMPF-3 device operated in the two different configurations, the one used in the Ref. [20] and the other one in the present investigation. Physically, the *SF* parameter controls the speed of plasma in both the axial and radial phases; and its constancy over a wide range of plasma focus devices indicates that these all devices operate at the same axial and radial speeds, and hence by inference they all have the same temperatures in the axial and radial phase [26]. Speed Factor is an empirical formulation between the maximum discharge current, anode radius and optimum deuterium gas pressure and it is used by many as an optimization tool for neutron yield maximizing, specially for initial electrode configuration design for any new plasma focus device [20].

The values for *SF* are 82 and 65 $\mathrm{kA}/\left(\mathrm{cm\ torr}^{0.5}\right)$ for the previous [20] and current experiments, respectively. Lee and Serban [26] tabulated the *SF* for different devices and concluded that the best *SF* typically lies in the range of 80–100 $\mathrm{kA}/\left(\mathrm{cm\ torr}^{0.5}\right)$. The SF values are used in designing the dimensions of electrode assembly of plasma focus device [27] and so, the first design of FMPF-3 device [20] was also based on typical SF value. However, in one of the best-optimized plasma focus devices (NX2 at NIE-NTU, Singapore), it was reported to be less than 60 when operated at 11 kV/270 kA with 12 mbar of deuterium [28]. Even in the present investigation, though the SF value is lower than the typical range it has higher neutron yield than the previous FMPF-3 version [20] which had *SF* in the best expected range. Characteristically, to attain the optimum PF design for maximum neutron yield requires other parameters, such as the insulator sleeve length, cathode and anode radii, anode length and material to be adjusted on a trial and error basis.

The typical current derivative and current signals from FMPF-3 are shown in Fig. 4. It may be noted that the start of the pinch phase, the starting time instant of sharp inverted peak in current derivative signal and sudden drop in current signal, is delayed compared to peak current position. For example, for 8 mbar D_2 operation, the quarter time period (T/4, the time to the peak discharge current)

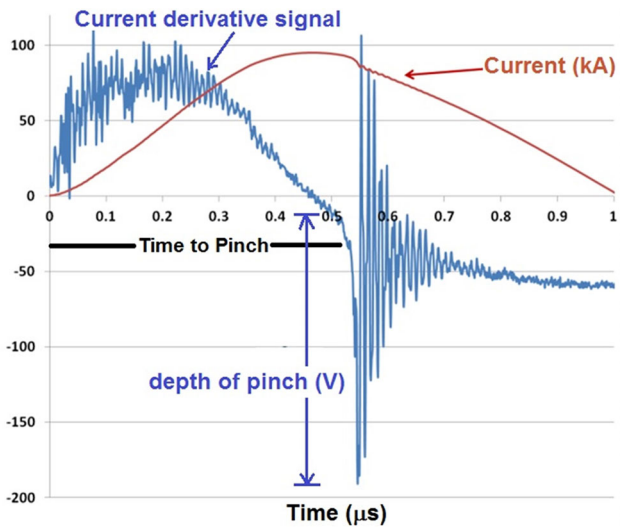

Fig. 4 Current derivative signal dI/dt (*blue colour trace*) from the Rogowski coil for measuring the time to pinch and depth of pinch. Discharge current $I(t)$ (*red colour trace*) obtained by numerical integration of dI/dt (Color figure online)

for the FMPF-3 discharge with all PSGs operating synchronously is about 420 ns while the average time to pinch for 55 shots is ~500 ns.

Our previous experimental results [29] on FMPF-3 with multiple PSGs show that the synchronization of switches has a significant effect on plasma evolution. The non-synchronized switching initiates an uneven discharge during the breakdown phase and remains such in axial and compression phases. It reduces pinch plasma density and temperature and consequently the fusion neutron yield. The reason for this significant delay may be that the PSGs are not working at their nominal operating parameters. In particular, the peak current through each PSG during the FMPF-3 discharge is about 25 kA, which is only 12.5 % of their maximum operating current of 200 kA. Consequently, the non-ideal commutation of the PSGs to their on-state may result in non-uniform breakdown condition across the insulator sleeve and consequently delay of well-defined current sheath formation in axial acceleration phase leading to significant delay in pinch phase compared to peak discharge current instant.

This additional time delay is also manifest when we try to fit the experimental current trace using Lee's code [25]. Firstly, $I(t)$ cannot be matched completely and secondly, it must be shifted back around 70 ns to match the radial phase and pinch current drop (as seen in Fig. 5). The Lee code then predicts an average neutron yield of 9.7×10^5, which is about half of the experimentally measured yield.

Neutron Yield for 10 mm Insulator Sleeve

The highest neutron emission efficiency in our lab was obtained on 3 kJ NX2 plasma focus device with the record neutron yield of 7×10^8 neutron/shot [30]. The NX2 device has the anode to insulator sleeve length ratio of about 2 which is half of the ratio used in current device. Hence, it was decided to increase the insulator sleeve length to 10 mm to achieve the anode to insulator sleeve length ratio of 2 with the aim of investigating the influence of this parameter on neutron yield. Again, a series of 55 shots (fired at ~0.2 Hz) were performed with pure deuterium and 1 % krypton seeding over the pressure range from 2 to 14 mbar. As seen in Fig. 6, for pure deuterium operation the average neutron yield for 10 mm sleeve reached its maximum value of about $Y_n = (2.2 \pm 0.2) \times 10^6$ n/shot at 6 mbar which is about 22 % higher than the maximum neutron of about $Y_n = 1.8 \times 10^6$ n/shot for 5 mm insulator sleeve at 8 mbar as seen in Fig. 5. The comparison of average neutron yield for pure deuterium operation for 5 mm sleeve (dark blue curve in Fig. 5) and 10 mm sleeve (light blue with cathode curve in Fig. 6) shows that for each of the operating deuterium gas pressures the average neutron yield for 10 mm sleeve was higher compared to 5 mm sleeve. This indicates that for pure deuterium operation the 10 mm insulator sleeve length FMPF-3 device is better optimized compared to 5 mm sleeve length geometry.

The key point to note from Fig. 6 is that for FMPF-3 device with 10 mm insulator sleeve length which is better optimized for pure deuterium operation with neutrons yields higher than 5 mm device, as discussed above, the average neutron yield decreases with 1 % Kr-seeding. It may be reminded that for non-optimized 5 mm sleeve the 1 % Kr-seeding led to the highest increase in average neutron yield. Hence, if the plasma focus device is fully or better optimized (such as the 10 mm sleeve FMPF-3) then the Kr-seeding may not result in increase in average neutron yield rather the yield may decrease. Beside, having a higher SF of 75 might be a good indication of leading to a better geometry design, although it cannot be the only reason.

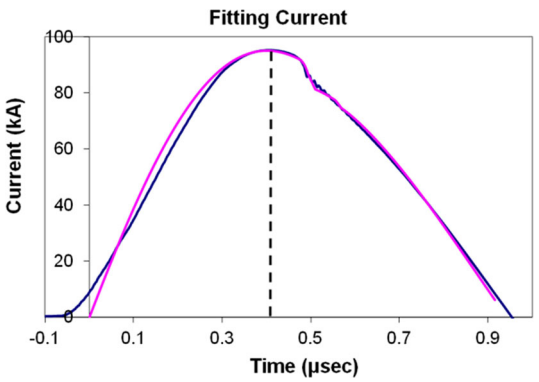

Fig. 5 The actual discharge current from FMPF-3 (*dark blue colour trace*) and the fitting current in Lee's code (*pink colour trace*) (Color figure online)

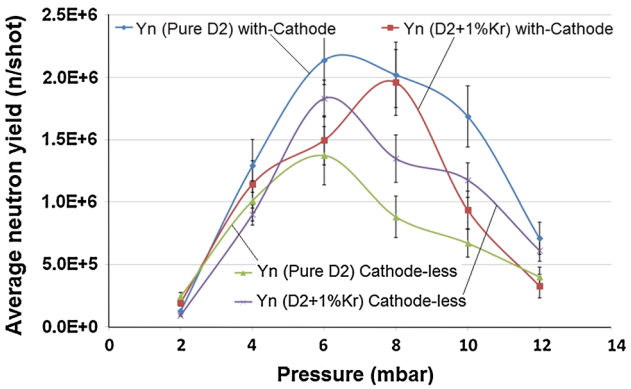

Fig. 6 Average neutron yield for 55 shots (per data point) with pure deuterium (*blue trace*) and 1 % Kr admixtures seeding (*red trace*) for 10 mm insulator sleeve (with cathode rods); and for cathode-less non-optimized geometry with pure deuterium (*green trace*) and 1 % Kr admixtures seeding (*purple trace*) for 10 mm insulator sleeve (Color figure online)

Neutron Yield for Cathode-Less Geometry

For the final group of experiments the cathode rods were removed to study the effect of this (presumably "non-optimized" or less-optimized geometry) on neutron yield. The variation of average neutron yield for cathode-less geometry for pure deuterium operation and 1 % Kr-seeding experiments (for 55 shots series at $\sim$0.2 Hz) as a function of gas pressure are shown in Fig. 6. The fact that cathode-less 10 mm insulator sleeve FMPF-3 device becomes a "non-optimized" configuration is confirmed by significantly reduced average neutron yield (green curve) for pure deuterium operation as the average neutron yield decreased by 36 % to $Y_n = (1.4 \pm 0.2) \times 10^6$ n/shot at 6 mbar in comparison to with-cathode geometry at the same pressure. The "non-optimized" cathode-less 10 mm insulator sleeve FMPF-3 geometry then exhibits the enhancement in average neutron yield with 1 % Kr-seeding with the peak average neutron yield increase by about 30 % to $Y_n = (1.8 \pm 0.2) \times 10^6$ n/shot. These results further support the idea that neutron yield enhancement obtained with krypton seeding is indicative of a non-optimized plasma focus geometry. It shows that the device's geometrical parameters, firstly, must be designed carefully and then improve them by trial and error to reach the optimum situation for highest neutron yield.

Figure 7 shows the depth of pinch, estimated from the depth of dip (inverted peak) in current derivative signal, for 10 mm insulator sleeve with cathode rods (optimized geometry) and cathode-less (non-optimized geometry) FMPF-3 device operation. It shows the reduction in the depth of pinch (refer to blue and red traces) by 1 % Kr seeding for the optimized 10 mm insulator sleeve geometry with-cathode rods was used. The non-optimized cathode-less geometry shows the increase in the depth of pinch (refer to green and purple traces) with krypton seeding. The results presented in Figs. 2 and 6 show that the depth of pinch increases with the krypton seeding if the geometry is non-optimized whereas it decreases for optimized geometry. A cross comparison of depth of pinch for three different geometries, shown in Fig. 3 and Fig. 7, shows that the depth of pinch is higher for non-optimized 5 mm insulator sleeve geometry. However, it is not appropriate to cross-compare the depth of pinch of two different geometries. For example, for PF geometries with different insulator sleeve lengths, the formation of current sheath at breakdown phase and consequently all other phases of plasma dynamics will be affected. This will also affect the volume, shape and duration of the final pinch column; making it inappropriate to cross-compare the electrical signals (which is controlled by the plasma dynamics) for different geometries. Hence, it can be concluded that for a given geometry the depth of pinch is related to degree of device optimization for neutron emission.

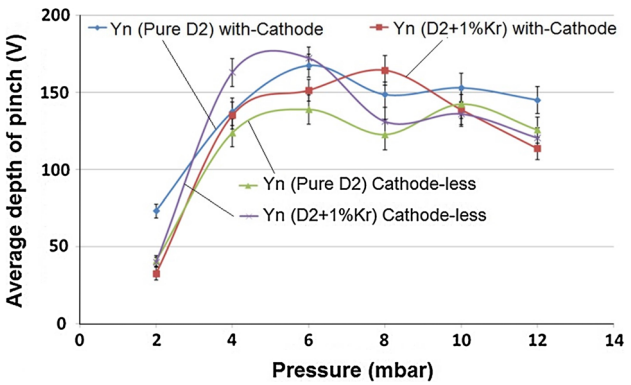

Fig. 7 Average depth of pinch for 55 shots (per data point) with pure deuterium (*blue trace*) and 1 % Kr admixtures seeding (*red trace*) for 10 mm insulator sleeve (with cathode rods); and for cathode-less non-optimized geometry with pure deuterium (*green trace*) and 1 % Kr admixtures seeding (*purple trace*) for 10 mm insulator sleeve (Color figure online)

Conclusion

In conclusion, our study shows that the krypton seeding in a deuterium plasma focus can increase the average neutron yield only for non-optimized devices whereas for well-optimized plasma focus devices, krypton seeding may lead to a reduced neutron yield. The Kr-seeding results in higher deuterium density in pinch column, for both "well-optimized" or "non-optimized" plasma focus devices, as higher bremsstrahlung radiation losses from high-Z plasma results in lower pinch plasma temperature and hence lower outward kinetic pressure and the confining magnetic pressure will compress the pinch plasma to tighter radius. The average deuteron energy reduces due to radiative cooling. For "non-optimized" plasma focus device both of these parameters, deuterium number density and average deuteron energy, are not optimized; whereas for the "optimized" plasma focus device these parameters are close to their optimized values. For "non-optimized" plasma focus device the increased deuterium number density effect dominates over the reduced average deuteron energy effect resulting in increased neutron yield. For "optimized" device the relative decrease in average deuteron energy is higher or comparable to relative increase in deuterium number density upon Kr-seeding leading to decrease in neutron yield. Finally, for a PF device with given electrical parameters, krypton seeding of deuterium can be regarded as a useful tool for investigating how close to neutron-optimized the geometrical configuration of the PF electrode assembly is.

Acknowledgments This study was supported by AcRF Tier1 research Grant No. RP1/11RSR provided by Nanyang Technological University, Singapore.

References

1. J.W. Mather, Phys. Fluids **8**(2), 366 (1965)
2. N.V. Filippov, T.I. Filippova, *Plasma Physics and Controlled Nuclear Fusion Research* (U.S. Atomic Energy Commission, Oak Ridge, 1965), p. 270
3. S. Lee, Plasma Phys. Control. Fusion **50**, 105005 (2008)
4. B.L. Bures, M. Krishnan, R.E. Madden, F. Blobner, IEEE Trans. Plasma Sci. **38**(4), 667 (2010)
5. R. Verma, R.S. Rawat, P. Lee, M. Krishnan, S.V. Springham, T.L. Tan, Plasma Phys. Control. Fusion **51**, 075008 (2009)
6. A.R. Babazadeh, M.V. Roshan, H. Habibi, A. Nasiry, M. Memarzadeh, A. Banoushi, M. Lamehi, S.M. Sadat Kiai, Braz. J. Phys. **32**(1), 89–94 (2002)
7. K.N. Koshelev, V.I. Krauz, N.G. Reshetniak, R.G. Salukvadze, Y.V. Sidelnikov, E.Y. Khautiev, J. Phys. D Appl. Phys. **21**(12), 1827 (1988)
8. J.S. Brzosko, V. Nardi, Phys. Lett. A **155**, 162–168 (1991)
9. W. Kies, G. Decker, U. Berntien, Y.V. Sidelnikov, D.A. Glushkov, K.N. Koshelev, D.M. Simanovskii, S.V. Babashev, Plasma Sources Sci. Technol. **9**, 27 (2000)
10. W. Kies, B. Lucas, P. Rowekamp, F. Schmitz, G. Ziethen, G. Decker, Plasma Sources Sci. Technol. **7**, 21 (1998)
11. V.V. Vikherev, S.I. Braginski, Rev. Plasma Phys. **10**, 425 (1986)
12. R. Verma, P. Lee, S. Lee, S.V. Springham, T.L. Tan, R.S. Rawat, M. Krishnan, Appl. Phys. Lett. **93**, 101501 (2008)
13. J.W. Shearer, Phys. Fluids **19**, 1426 (1976)
14. J. Bailey, A. Fisher, N. Rostoker, J. Appl. Phys. **60**, 1939 (1986)
15. S.V. Springham, A. Talebitaher, P.M.E. Shutler, S. Lee, R.S. Rawat, P. Lee, Appl. Phys. Lett. **101**, 114104 (2012)
16. M.A. Mohammadi, S. Sobhanian, R.S. Rawat, Phys. Lett. A **375**(33), 3002 (2011)
17. R. Aliaga-Rossel, P. Choi, IEEE Trans. Plasma Sci. **26**(4), 1138 (1998)
18. R. Verma, M.V. Roshan, F. Malik, P. Lee, S.V. Springham, T.L. Tan, S. Lee, M. Krishnan, R.S. Rawat, Plasma Sources Sci. Technol. **17**(4), 045020 (2008)
19. R. Verma, R.S. Rawat, P. Lee, S. Lee, S.V. Springham, T.L. Tan, M. Krishnan, Phys. Lett. A **373**, 2568–2571 (2009)
20. R. Verma, R.S. Rawat, P. Lee, S.V. Springham, T.L. Tan, J. Fusion Energ. **32**(1), 2–10 (2013)
21. A. Talebitaher, S.V. Springham, R.S. Rawat, P. Lee, Nucl. Inst. Methods Phys. Res. A **659**, 361 (2011)
22. R. Verma, PhD thesis, Nanyang Technological University (2010)
23. S. Lee, S.H. Saw, J. Ali, J. Fusion Energ. **32**, 42–49 (2012)
24. S. Lee, Aust. J. Phys. Aust **35**, 891–895 (1983)
25. S. Lee, Radiative Dense Plasma Focus Computation Package: RADPF (2012). http://www.plasmafocus.net
26. S. Lee, A. Serban, IEEE Trans. Plasma Sci. **24**(3), 1101 (1996)
27. S. Lee, S.H. Saw, R.S. Rawat, P. Lee, R. Verma, A. Talebitaher, S.M. Hassan, A.E. Abdou, M. Ismail, A. Mohamed, H. Torreblanca, Sh Al Hawat, M. Akel, P.L. Chong, F. Roy, A. Singh, D. Wong, K. Devi, J. Fusion Energ. **31**, 198–204 (2012)
28. A. Patran, R.S. Rawat, J.M. Koh, S.V. Springham, T.L. Tan, P. Lee, S. Lee, in Proceedings of 31st EPS Conference on Plasma Physics, London (2004)
29. A. Talebitaher, S.M.P. Kalaiselvi, S.V. Springham, P. Lee, T.L. Tan, R.S. Rawat, J. Fusion Energ. **34**, 794–801 (2015)
30. J.M. Koh, R.S. Rawat, A. Patran, T. Zhang, D. Wong, S.V. Springham, T.L. Tan, S. Lee, P. Lee, Plasma Source Sci. Technol. **14**, 12 (2005)